

- mutual effect to displace each other from the binding site. *Am. J. Drug Dis. Dev.*, 2011, **1**, 220–230.
11. Samadi-Maybodi, A. and Hassani Nejad-Darzi, S. K., Simultaneous determination of paracetamol, phenylephrine hydrochloride and chlorpheniramine maleate in pharmaceutical preparations using multivariate calibration. *Spectrochim. Acta A*, 2010, **75**, 1270–1274.
  12. El-Gamel, N. E. A., The interactions of metal ions with nonsteroidal anti-inflammatory drugs (oxicams). *J. Coord. Chem.*, 2009, **62**, 2239–2260.
  13. Geyer, M., Antimalarial drug combination therapy: Report of a WHO Technical Consultation, World Health Organization, Geneva, 2001.
  14. Parhi, P., Mohanty, C. and Sahoo, S., Nanotechnology-based combinational drug delivery: an emerging approach for cancer therapy. *Drug Discov. Today*, 2012, **17**, 1044–1052.
  15. Skolnik, N. S., Beck, J. D. and Clark, M., Combination antihypertensive drugs: recommendations for use. *Am. Fam. Physician*, 2000, **61**, 3049–3056.
  16. Stolarczyk, M., Maslanka, A., Apola, A. and Krzek, J., Analysis of hypotensive compounds occurring in complex agents. *Acta Pol. Pharm.*, 2010, **67**, 441–454.
  17. Hajian, R., Shams, N. and Rad, A., Application of H-Point standard addition method for simultaneous spectrophotometric determination of hydrochlorothiazide and propranolol. *J. Braz. Chem. Soc.*, 2009, **20**, 860–865.
  18. Narasimham, L. Y. S. and Barhate, V. D., Development and validation of stability indicating UPLC method for the simultaneous determination of beta-blockers and diuretic drugs in pharmaceutical dosage forms. *J. Chem. Metrol.*, 2010, **4**, 1–20.
  19. Sarafraz-Yazdi, A., Abedi, M. R., Eshaghi, Z. and Kakhki, J. F., Simultaneous determination of metoprolol and propranolol using chemometric assisted spectrophotometry and high performance liquid chromatography. *Int. J. Pharm. Biol. Sci.*, 2012, **3**, 532–542.
  20. Sampson, L., Wilson, B. and Hou, H. J. M., Gas chromatography-mass spectrometric analysis of forensic drug flunitrazepam upon exposure to UV irradiation. *J. Forensic Res.*, 2013, **4**, 1–4.
  21. Angier, M. K., Lewis R. J., Chaturvedi, A. K. and Canfield, D. V., Gas chromatographic mass spectrometric differentiation of atenolol, metoprolol, propranolol and an interfering metabolite product of metoprolol. *J. Anal. Toxicol.*, 2005, **29**, 517–521.
  22. Knoth, H., Petry, T. and Gartner, P., Differential pulse polarographic investigation of the antifungal drugs itraconazole, ketoconazole, fluconazole and voriconazole using a dropping mercury electrode. *Pharmazie*, 2012, **67**, 987–990.
  23. Jain, R. and Sharma, R., Voltammetric quantification of anti-hepatitis drug adefovir in biological matrix and pharmaceutical formulation. *J. Pharm. Anal.*, 2012, **2**, 98–104.
  24. Sikkander, M., Vedhi, C. and Manisankar, P., Cyclic voltammetric determination of 1, 4-Dihydro pyridine drugs using MWCNTs modified glassy carbon electrode. *Der Chem. Sin.*, 2012, **3**, 413–420.
  25. Suntornsuk, L., Capillary electrophoresis in pharmaceutical analysis: a survey on recent applications. *J. Chromatogr. Sci.*, 2007, **45**, 559–577.
  26. Srivastava, S. and Coutinho, E., Adrenergic antagonist propranolol as a novel, effective spermicide: an NMR study. *Int. J. Pharm. Pharm. Sci.*, 2010, **2**, 196–200.
  27. Holzgrabe, U., Deubner, R., Schollmayer, C. and Waibel, B., Quantitative NMR spectroscopy applications in drug analysis. *J. Pharm. Biomed. Anal.*, 2005, **38**, 806–812.
  28. Venkatesan, P., Dharuman, C. and Gunasekaran, S., A comparative study of principal component regression and partial least squares regression with application to FTIR diabetes data. *Indian J. Sci. Technol.*, 2011, **4**, 740–746.
  29. Darwish, H. W. and Backeit, A. H., Multivariate versus classical univariate calibration methods for spectrofluorimetric data: application to simultaneous determination of olmesartan medoxamil and amlodipine besylate in their combined dosage form. *J. Fluoresc.*, 2013, **23**, 79–91.
  30. Mevik, B. H. and Wehrens, R., The pls package: principal component and partial least squares regression in R. *J. Stat. Softw.*, 2007, **18**, 1–23.
  31. Lindberg, W., Persson J. A. and Wold, S., Partial least squares method for spectrofluorimetric analysis of mixtures of humic acid and ligninsulfonate. *Anal. Chem.*, 1983, **55**, 643–648.
  32. Kramer, R., *Chemometric Techniques for Quantitative Analysis*, Marcel Dekker, New York, 1998.

ACKNOWLEDGEMENT. This work is financially supported by SERB (DST), New Delhi (CS-212/2012).

Received 1 October 2014; revised accepted 10 December 2014

## Numerical analyses of laboratory-modelled reinforced stone column

Yogendra Tandel<sup>1,\*</sup>, Mohsin Jamal<sup>2</sup>, Chandresh Solanki<sup>3</sup> and Atul Desai<sup>3</sup>

<sup>1</sup>GIDC Degree Engineering College, Navsari 396 439, India

<sup>2</sup>U.V. Patel College of Engineering, Mehsana 384 012, India

<sup>3</sup>S.V. National Institute of Technology, Surat 395 007, India

**A stone column develops its vertical load carrying capacity by the lateral pressure provided by the surrounding soil. In very soft clay ( $C_u \leq 15$  kPa), the stone column may not derive its load carrying capacity. Sometimes the formation of stone column is doubtful. In such cases, the stone column may be wrapped with geosynthetic peripherally (circumferentially). Normally, reinforced stone columns are used for widely spread areas like air tank foundation and embankment in which they are confined by surrounding the columns. The performance of a small group of reinforced stone columns is complex. This communication focuses on the numerical modelling of a small group of laboratory-modelled reinforced stone columns. The study is carried out considering parameters like area replacement ratio (ARR), stiffness of reinforcement material and reinforcement length. The performance of reinforced stone column group is discussed in terms of bearing ratio, ( $q/C_u$ )-settlement ratio, stress concentration factor and lateral deformation. The results of numerical analyses indicate that ARR and stiffness of geosynthetic are the governing parameters for enhancing the performance of reinforced stone column. The performance of partial reinforced stone column is close to that of a fully reinforced stone column.**

\*For correspondence. (e-mail: tandel.yogendra@gmail.com)

**Keywords:** Ground improvement, load carrying capacity, numerical analysis, stone column.

STONE column is one of the popular ground improvement methods used to enhance settlement, bearing capacity and lateral flow of soft soils. But in very soft clay, stone column material may squeeze into the clay, which may clog (or block) voids of the stone column or construction of stone column may be in doubt. To overcome these problems, an individual stone column may be reinforced with a suitable geosynthetic in periphery. Van Impe was the first to suggest the provision of geosynthetic reinforcement. In 1989, he proposed the analytical solution for the axial load carrying capacity of reinforced stone column based on hoop force theory<sup>1</sup>. Kempfert<sup>2</sup> reported the first use of reinforced stone column for strengthening 5 m high embankment foundation. Raithel *et al.*<sup>3</sup> reported the largest application of reinforced stone column for the dyke foundation improvement at Elbe river bank in Hamburg, Germany for the production site of Airbus A380.

Stone columns are often being applied for wide spreader load, such as oil tank or an embankment foundation, resting on a large array of stone columns, in which individual stone columns are surrounded by others. Therefore, all columns are equally confined (or constrained) on all sides. But, a stone column can also being applied in a limited group for supporting small area footing. The behaviour of a small group of stone columns is complex as peripheral columns are subject to loss of lateral confinement.

Many researchers have reported the performance of single and a group of reinforced stone columns through laboratory model tests. Based on the laboratory triaxial tests on single reinforced stone column through unit cell approach, Bauer and Nabil<sup>4</sup> concluded that the reinforced stone column has increased the stiffness, which in turn increases the load carrying capacity of the column. Malarvizhi and Ilamparuthi<sup>5</sup> performed laboratory model tests on single end bearing and floating reinforced stone column in soft clay with different nets in constrained condition. Trunk *et al.*<sup>6</sup> performed medium-scale unconfined compression tests on geogrid wrapped stone columns under static and dynamic loading condition. Ayadat and Hanna<sup>7</sup> exposed the effectiveness of the reinforcement of stone column in collapsible soils through laboratory triaxial tests based on unit cell approach. The improvement in load carrying of reinforced stone column under non-monotonic vertical load was reported by Di Prisco *et al.*<sup>8</sup>. Lee *et al.*<sup>9</sup> studied the load carrying capacity and failure mechanism of geogrid reinforced stone column by laboratory model tests in constrained condition. Murugesan and Rajagopal<sup>10,11</sup> performed laboratory model tests on single and a group of stone columns based on unit cell approach to study the effects of columns diameter, geosynthetic stiffness and length of reinforcement on the load carrying capacity of geosynthetic

reinforced stone columns. They reported that the performances of partially reinforced columns approached that of fully reinforced columns. Murugesan and Rajagopal<sup>12</sup> developed a special test set-up to simulate the behaviour of reinforced stone column under embankment loading. The performances of geosynthetic reinforced stone columns were observed to be superior compared to those of ordinary stone column. Gniel and Bouazza<sup>13</sup> provided comparative study on the behaviour of single and a group of reinforced stone columns in triaxial cell based on unit cell approach and observed a steady reduction in vertical strain with increasing reinforcement length. Their studies were based on unit cell approach. Wu and Hong<sup>14</sup> performed triaxial compression tests on unreinforced and reinforced single stone columns using unit cell approach. Their study indicated that reinforcement induced apparent cohesion to the stone column material. Gniel and Bouazza<sup>15</sup> proposed a method for a construction of geogrid reinforced stone column based on the medium-scale laboratory unconfined compression tests.

Numerous researchers have carried out numerical analyses on reinforced stone column. Two-dimensional axisymmetric finite element analyses of single ordinary and reinforced stone columns were conducted by Murugesan and Rajagopal<sup>16</sup>. They argued that the depth of reinforcement equal to twice the diameter of the stone column is sufficient to substantially increase its load carrying capacity. Based on two-dimensional finite element analyses on single reinforced stone column, using axisymmetric finite element modelling of single reinforced stone column, Malarvizhi and Ilamparuthi<sup>17</sup> observed that the increase in load carrying capacity of the column was not effective beyond length to column diameter ratio of 10 and geogrid stiffness over 2000 kN/m. Khabbazian *et al.*<sup>18</sup> performed three-dimensional finite element analyses on single reinforced stone column. They postulated that it is more efficient to select reinforcement with higher stiffness rather than to improve the stone column material. Yoo and Kim<sup>19</sup> compared the different modelling approaches (i.e. axisymmetric, 3D unit cell and fully 3D) for the performance of reinforced stone column embedded in embankment foundation. They observed that the results of 3D unit cells were in good agreement with those of the fully 3D model for a reinforced stone column. Yoo<sup>20</sup>, based on full three-dimensional finite elements modelling of an embankment resting on geosynthetic reinforced stone column, argued that full reinforcement may be necessary to ensure maximum settlement reduction when implementing geosynthetic reinforced stone column under an embankment loading condition.

Although the behaviour of single and a group of reinforced stone columns has been studied by many researches using laboratory and numerical models, they were based on unit cell approach, which is used to simulate the behaviour of stone column under constrained

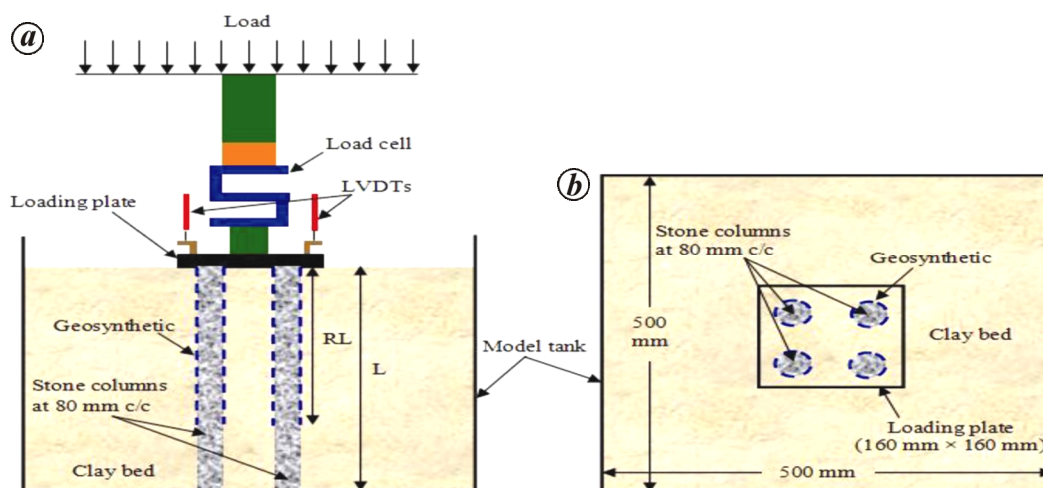


Figure 1. Schematic diagram of load test on a small group of stone columns: *a*, Front elevation; *b*, Plan.

condition. However, stone columns are often applied in a small group, which is not constrained. Nevertheless, to the knowledge of the present authors, no information can be found on studies of reinforced stone column in a small group. The objectives of the present study are therefore as follows:

- To check the feasibility of application of a small group of reinforced stone columns for a building foundation.
- To verify the experimental model test results with a three-dimensional finite element result.
- To compare the behaviour of partially reinforced stone column and fully reinforced stone column.
- To check the influence of stiffness of reinforcement; area replacement ratio (ARR) on load deformation behaviour of treated soil bed.

To achieve the above objectives, the following scopes are identified:

- The feasibility of an application of a small group of reinforced stone columns is studied by preparing three-dimensional finite element model by modelling reinforcement as a geogrid element capable of taking tensile force only and soil and stone column according to Coulomb failure criteria.
- The behaviour of a small group of reinforced stone columns is judged based on the output parameters, namely bearing ratio, settlement ratio, stress concentration factor and lateral deformation.
- The influence of reinforcement on the performance of a small group of reinforced stone columns is evaluated by adopting different reinforcement stiffness values.
- The effect of ARR of stone column is studied by adopting two different diameters, namely 25 and 40 mm.
- The performance of partial reinforced stone column is studied by taking reinforcement length equal to 50% of stone column length.

The present study is focused on feasibility of the utilization of reinforced stone column as a foundation of small building footings to minimize the failure of structures supported on shallow foundation. The study also encompasses the efficient use of partially reinforced stone columns for the designed load carrying capacity of the foundation instead of applying fully reinforced stone column which eventually results into economy of the project.

All the experiments were conducted on model tank of size  $0.5 \text{ m} \times 0.5 \text{ m} \times 0.40 \text{ m}$ . Model test with steel plate size of  $0.16 \text{ m} \times 0.16 \text{ m}$  was used to load clay bed treated with stone columns. Four stone columns were spaced in square grid pattern at 180 mm, centre-to-centre. Stone columns of diameter 0.02 and 0.04 m were used, which provided ARR of 7.67% and 19.63% respectively. Here, ARR is defined as the ratio between area of stone columns and area of loading plate. The length of stone columns ( $L$ ) was kept equal to thickness of the clay bed. Tests were also performed with different lengths of reinforcement (RL). In this article, stone column without reinforcement is denoted as OSC and that with reinforcement as RSC. The schematic diagram of load test arrangement is shown in Figure 1.

For the preparation of clay bed, soil particles of size less than 2 mm were used. Table 1 summarizes the geotechnical properties of clay. Sands passing from 4.75 mm sieve was used to prepare the stone columns. It is classified as poorly graded sand. The other properties of sand are listed in Table 1. The modules of elasticity of clay and sand were determined based on the result of triaxial test. The modules of elasticity reported in Table 1 are based on confining pressure existing the model tests.

Three different types of geosynthetics were used for reinforcement. They are net, non-woven and woven geotextile. The reinforcement in the form of cylindrical tube was prepared by bonding the edges of the geosynthetics

with epoxy resin keeping 30 mm overlap. The properties of different geosynthetics are depicted in Table 2. In the present study, clay bed thickness is kept as 400 mm.

The required amount of water and soil was mixed and kept for 48 h in order to achieve uniform consistency. The soil paste was placed in a tank in 50 mm thick layers by moulding with hand. For installation of the stone column, displacement method was used in which steel casing pipe was pushed into the clay bed along with a base plate having circular groove to facilitate the casing pipe. The stone columns were constructed in 50 mm thick layers by applying equal amount of compaction energy to each layer to maintain uniform density of the columns. In case of reinforced stone column, geosynthetics were wrapped around the casing pipe.

Load was applied by loading plate placed on a group of stone column-treated clay beds. The displacement was measured using a linear variable displacement transducer (LVDTs).

Numerical analyses of stone column-treated beds were carried out using the PLAXIS 3D Package<sup>21</sup>, to compare the load–deformation results with the laboratory model test results. For this, three-dimensional finite-element models of exactly the same size as the laboratory models were prepared and analysed.

Roller supports were used on the vertical faces of the clay bed. The bottom face of the clay bed was considered as fixed. Mohr–Coulomb failure criterion was adopted for stone column and clay having linearly elastic perfectly plastic behaviour. The geosynthetics were modelled as geogrid element available in PLAXIS 3D having axial stiffness only. The input parameters for clay and stone column material (unit weight, cohesion, elastic modulus,

angle of internal friction, Poisson ratio and dilatancy angle) are given in Table 1.

The zone of the interface between stone column–geosynthetics and geosynthetics–clay is one with very high difference in magnitude in Young’s modulus of the order of ten times or more. In addition, the shear strength properties of this zone depend on the method of installation of stone columns. The above two properties of the interface are difficult to quantify. During the loading stage the stone column induces lateral displacement of clay in the lateral direction, where the shearing phenomenon along the interface is nearly absent. Hence, to make the analyses simple, the interface element is not considered. The mesh was refined in the region of the column–soil interface to increase the accuracy of the predictions. Figure 2 shows the mesh discretization adopted for a group of stone columns.

Application of this material model was verified with the published results of Ambily and Gandhi<sup>22</sup>, where in Mohr–Coulomb model was used to analyse the stone column and clay bed. The test tank used in their experiments was 210 mm in diameter and height of clay bed was 450 mm. In their analysis, undrained shear strength of clay varied from 7 to 30 kPa. A stone column of diameter 100 mm and height 450 mm was made at the centre of the clay bed and loaded with a plate of diameter equal to that of the stone column. Properties of clay and stones are shown in Table 3. An axisymmetry analysis was carried out using Mohr–Coulomb’s criterion for clay and stones.

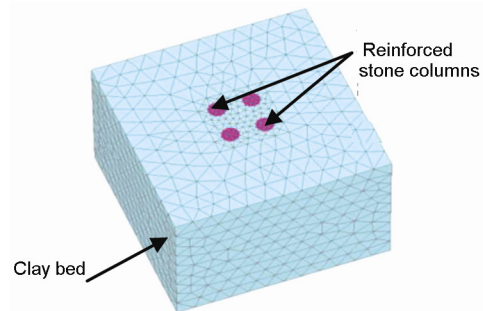


Figure 2. Typical finite element mesh used in the analysis of a group of stone columns.

Table 1. Properties of soft clay and stone column material

Parameters	Properties	
	Soft clay	Stone column
Liquid limit (%)	46	–
Plasticity index (%)	29	–
Water content (%)	36	–
Dry unit weight (kN/m <sup>3</sup> )	12.50	16
Bulk unit weight (kN/m <sup>3</sup> )	17	–
Undrained cohesion (kPa)	9	–
Angle of internal friction (degrees)	–	30
Elastic modulus (kPa)	106	1886
Poisson ratio	0.49	0.30

Table 2. Properties of geosynthetics

Type of geosynthetics	Properties		
	Net	Non-woven geotextile	Woven geotextile
Ultimate tensile strength (kN/m)	2.6	7.5	12
Strain at ultimate strength (%)	60	55	35
10% secant modulus (kN/m)	6	10	23

Table 3. Properties of materials used for the validation of material model<sup>22</sup>

Parameters	Properties	
	Clay	Stone
Modulus of elasticity (kPa)	5500	55,000
Poisson ratio	0.42	0.3
Shear strength (kPa)	30	–
Angle of internal friction (degrees)	–	43
Dilation angle (degrees)	–	10
Dry unit weight (kN/m <sup>3</sup> )	15.56	16.62
Bulk unit weight (kN/m <sup>3</sup> )	19.45	–

Figure 3 compares the results of a numerical analysis carried out in the present study with both the experimental and numerical results of Ambily and Gandhi<sup>22</sup>, which match well. Mustafa *et al.*<sup>23</sup> have also adopted the same constitutive model for the stone column and soft clay bed. Therefore, this model was adopted for further analyses.

In this section, the bearing ratio ( $q/C_u$ ) – settlement ratio ( $S/B$ ) response obtained by laboratory model tests and numerical analyses is compared for untreated clay bed, clay bed treated with ordinary and reinforced stone columns (Figure 4). Here, bearing ratio is defined as the ratio between load carrying capacity ( $q$ ) at 50 mm settlement and undrained cohesion of clay ( $C_u$ ) whereas settlement ratio is defined as the ratio between settlement of footing ( $S$ ) and footing width ( $B$ ).

It can be seen from the figure that experimental and numerical results are comparable. The maximum error observed between experimental and numerical analyses results is about 15%.

In the following sections, the results from numerical analyses are presented and discussed for the influence of reinforcement, ARR, stiffness of reinforcement and length of reinforcement (RL) on the performance of a group of stone columns.

The bearing ratio versus settlement ratio of untreated clay bed, clay bed treated with ordinary stone column and reinforced stone column is illustrated in Figure 5 for ARR = 19.63% and full reinforcement length (i.e. RL/L = 1). Figure indicates that bearing ratio of the stone

column increases remarkably by provision of geosynthetic reinforcement. But the clay bed treated with ordinary stone column does not improve bearing ratio significantly. For instance, increase in bearing ratio w.r.t. untreated clay bed at  $S/B = 0.27$  (i.e. at 50 mm settlement) is about 15% with ordinary stone column, but is about 152% for reinforced stone column.

In order to understand the load transfer mechanism in the clay bed improved with stone columns, the stress concentration factor ( $n$ ) is plotted against the depth. The stress concentration factor is defined as the ratio of the stress on the stone column to that of the soil. The stress concentration occurs in the stone column due to the higher relative stiffness of the column to the soil. The higher the stress concentration factor, the higher the stress on the column compared to the soil. In Figure 6 the stress concentration factor is plotted with depth for OSC and RSC. The values of the stress concentration factor vary with depth. It is also seen that the stress concentration factor with RSC is about 4.6 times more than OSC. This indicates that RSC behaves similar to flexible columnar elements, which carry a higher percentage of total load and transfer a smaller fraction to the surrounding soil. As the degree of load transfer between the column and soil depends largely on the modular ratio between the

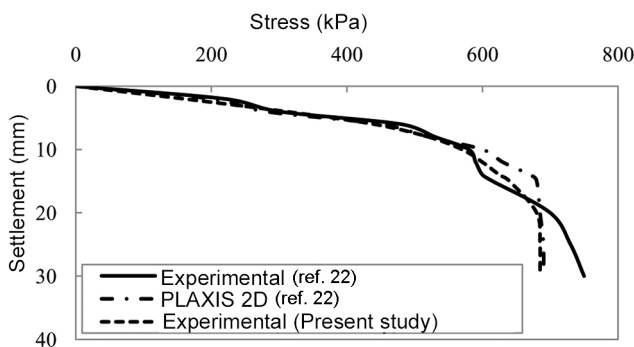


Figure 3. Validation of FEM with Ambily and Gandhi<sup>22</sup>.

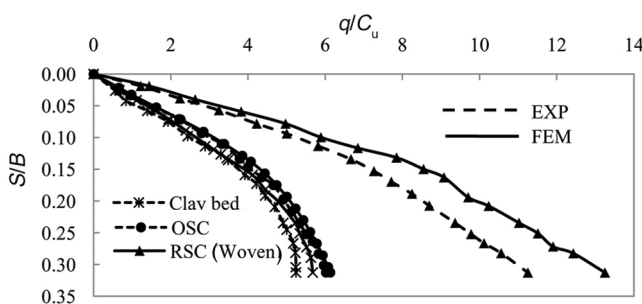


Figure 4. Comparison of experimental and numerical analyses results for untreated clay bed, OSC and RSC (woven).

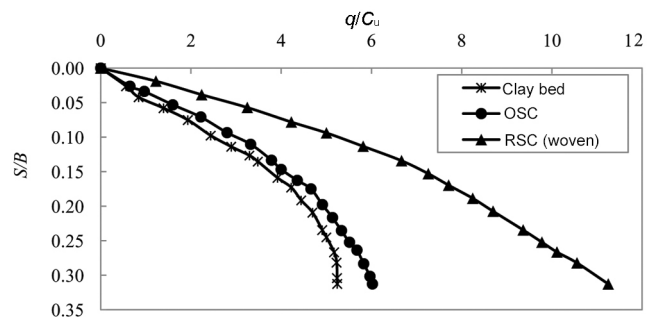


Figure 5.  $q/C_u$  versus  $S/B$  for OSC and RSC (woven) with RL/L = 1.

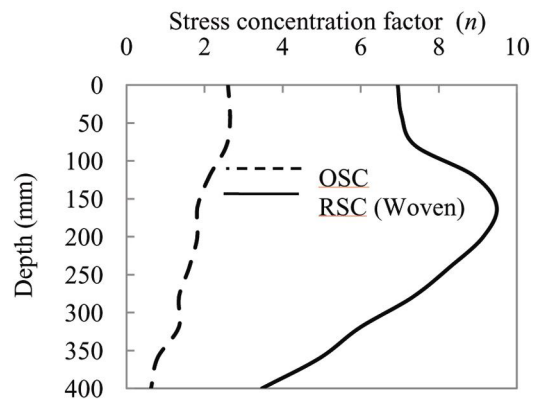


Figure 6. Influence of reinforcement on stress concentration factor with ARR = 19.63%.

stone column and the surrounding soil, the stress concentration factor is thus expected to be larger for RSC than for OSC.

Lateral deformation of OSC and fully reinforced stone column (i.e.  $RL/L = 1$ ) with woven geotextile for ARR = 19.63% is illustrated in Figure 7. From the figure, it can be seen that lateral deformation of OSC tends to sharply increase with length up to 6.38 mm at  $2.75d$  ( $d$  is the stone column diameter), below the top of the stone column, after which it decreases with depth. When reinforcing the stone column, the lateral deformation is considerably reduced primarily because of the additional lateral confinement by the reinforcement.

To check the influence of ARR on the performance of reinforced stone column, two different diameters (25 mm and 40 mm) were considered to be placed at 80 mm centre-to-centre, which corresponds to ARR of 7.67% and 19.63% respectively.

In Figure 8, bearing ratio is plotted against settlement ratio for different ARR of ordinary and reinforced stone column. From the figure, it is clear that response of a group of ordinary stone columns is almost the same. But for reinforced stone column, bearing ratio increases with increase in ARR for a given amount of settlement ratio.

The stress at 10% strain with ARR is shown in Figure 9 for different reinforcement materials. The figure indicates that load carrying capacity increases with increase

in ARR for reinforced stone column. But maximum amount of increase is obtained for stone column reinforced with woven geotextile. For instance, percentage increase in load carrying capacity by changing ARR from 7.67 to 19.63 is 12, 24 and 27 for RSC (net), RSC (non-woven) and RSC (woven) respectively.

From the present study, it can also be concluded that stress on the RSC increases with increases in diameter of the stone column. This finding is not in line with the previous findings of Murugesan and Rajagopal<sup>16</sup>, and Khabbazian *et al.*<sup>18</sup>, in which they reported that stress on reinforced stone column decreases with increase in diameter of the column. In their research work, the influence of stone column diameter on the behaviour of RSC was studied by applying the load to the column diameter only. Increase in the diameter of the column has a negative effect on the performance of each single RSC due to decrease in the effectiveness of its reinforcement; it leads to an increase in ARR, which has a greater influence on the performance of RSC and results in the improvement in overall performance of a group of RSCs. Applying the load only to the stone column diameter ignores the positive effect of the increase in the ARR on the overall performance.

Figure 10 shows lateral deformation profiles along the depth of the stone column for different replacement ratios, determined using numerical analyses. It can be

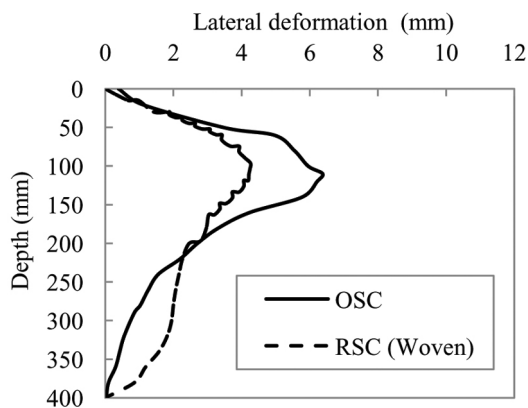


Figure 7. Lateral deformation versus depth for OSC and a RSC (woven) with ARR = 19.63% and  $RL/L = 1$ .

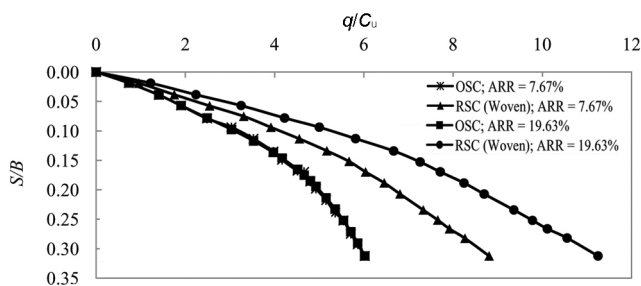


Figure 8.  $q/C_u$  versus  $S/B$  for OSC and RSC (woven) with  $RL/L = 1$ .

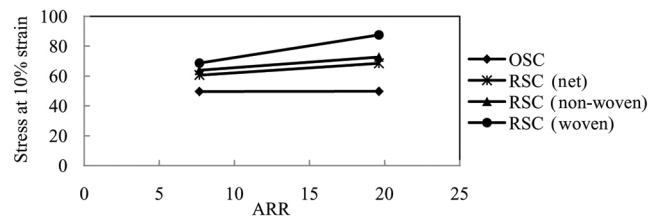


Figure 9. Effect of ARR on the performance of group of OSC and RSC with  $RL/L = 1$ .

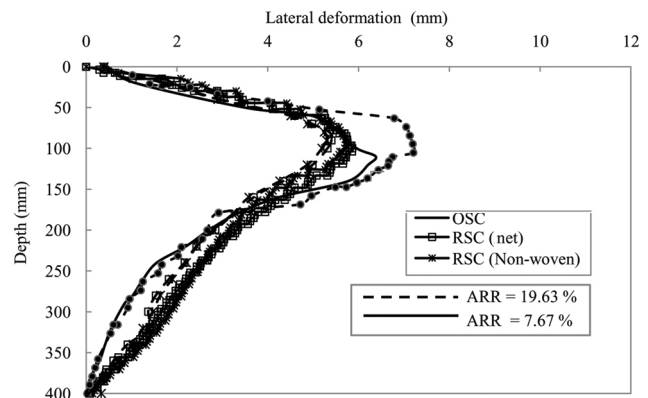


Figure 10. Lateral deformation versus depth for OSC, RSC (net) and RSC (non-woven) at a vertical settlement of 50 mm with  $RL/L = 1$  and different ARR.

seen that lateral deformation of OSC decreases with increase in ARR. However, in RSC with an increase in ARR or increase in diameter of the column, lateral deformation increase. This may be due to the lower confinement pressure developed in the bigger diameter column.

To incorporate the influence of stiffness of reinforcement, three different geosynthetics, namely net, non-woven and woven geotextile having 10% secant modulus of 6, 10 and 23 kN/m respectively, were used. From Figure 11, it is clear that with increase in modulus of reinforcement, bearing ratio increases. This may be due to increase in confinement pressure. It is observed from Figure 12 that as modulus increase from 6 to 10 kN/m, the increase in stress is not appreciable, but after 10 kN/m, stress increases rapidly. For example, with increase in secant modulus from 6 to 10 kN/m, stress increase by 12%, but as secant modulus changes from 10 to 23 kN/m, stress increase by 51%.

The stress concentration factor is plotted in Figure 13 against 10% secant modulus of geosynthetic reinforcement for ARR = 19.63% and RL/L = 1 (i.e. fully reinforced column). The values of stress concentration factor have a tendency to increase with an increase in the modulus of the reinforcement. The increase in stress concentration is more in the columns reinforced with stiffer geosynthetic material. For example, the stress concentration factor for stone column reinforced with woven geotextile is 2.22 and 3.58 times larger than OSC and RSC

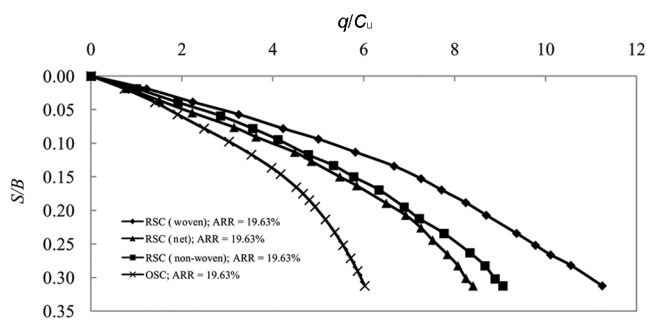


Figure 11.  $q/C_u$  versus  $S/B$  for OSC and RSC with different types of reinforcement for  $RL/L = 1$ .

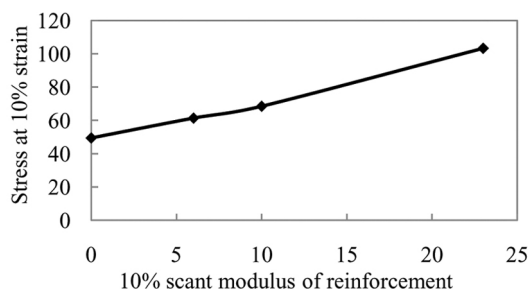


Figure 12. Effect of modulus of reinforcement on the performance of a group of RSCs with  $RL/L = 1$  and ARR = 19.63%.

(net) respectively. This indicates that the stone column reinforcement increases the amount of load transferred to stone columns, which results in the reduction in settlement of treated bed.

The lateral deformation of the stone column for ARR = 19.63% and  $RL/L = 1$  is illustrated in Figure 14 for different reinforcement stiffness values. From the figure, it can be seen that the lateral deformation of the stone column decreases with increase in reinforcement stiffness due to lateral confinement. The decrease in lateral deformation is significant for stone column reinforced with woven geotextile than with net and non-woven geotextile.

The common failure mechanism of stone column is bulging (or lateral deformation). Hence, reinforcement may be required near the top portion where the lateral deformation is predominant. To check the influence of length of reinforcement (RL), stone columns were reinforced up to half the length of column (i.e.  $RL/L = 0.50$ ) and up to full column length (i.e.  $RL/L = 1$ ). The bearing ratio versus settlement ratio of stone column reinforced with different geotextiles is shown in Figure 15 for ARR = 19.63% and different reinforcement lengths. The figure indicates that bearing ratio increases with increase

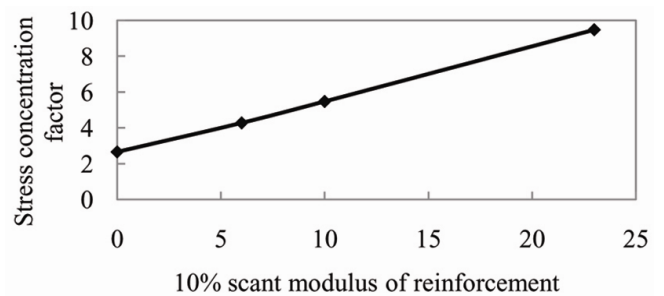


Figure 13. Effect of modulus of reinforcement on stress concentration factor with ARR = 19.63% and  $RL/L = 1$ .

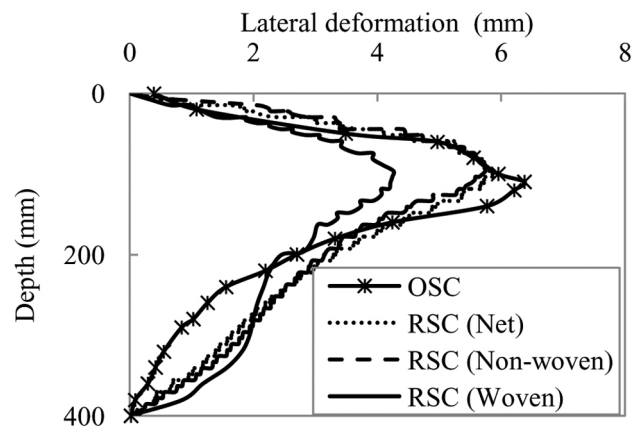


Figure 14. Lateral deformation versus depth for stone column reinforced with different types of reinforcement, at a vertical settlement of 50 mm with  $RL/L = 1$  and ARR = 19.63%.

in reinforcement length, irrespective of the type of reinforcement. But the increase in bearing ratio is not significant as RL/L ratio changes from 0.50 to 1. For instance the maximum increase in bearing ratio is observed to be 14%.

Figure 16 shows the variation of stress concentration factor (obtained from numerical analysis) with RL/L ratios for different stiffness of reinforcement values and ARR = 19.63%. It indicates that with decreasing reinforcement length the stress concentration factor reduces, thereby increasing the settlement ratio.

The lateral deformation with depth is plotted in Figure 17 for the different reinforcement lengths and reinforcement stiffness values with ARR = 19.63%. The figure indicates that with partial reinforcement of the column up to half-length (i.e. RL/L = 0.50), the lateral deformation occurs at the junction of reinforced and unreinforced

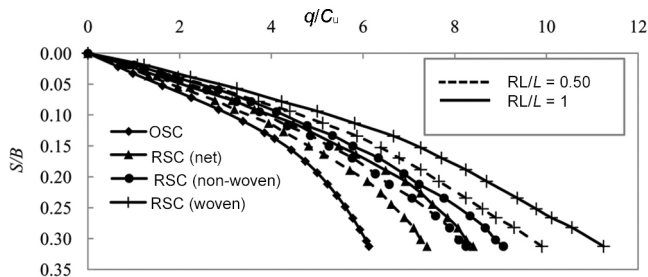


Figure 15.  $q/C_u$  versus  $S/B$  for OSC and RSC with ARR = 19.63% and different reinforcement lengths.

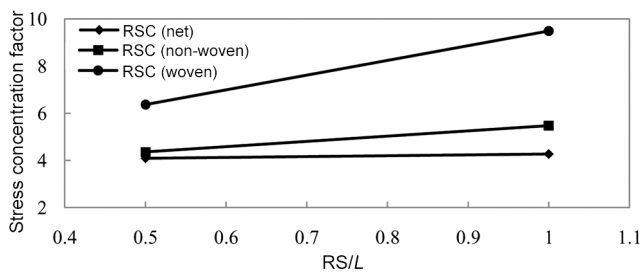


Figure 16. Effect of reinforcement length on stress concentration factor.

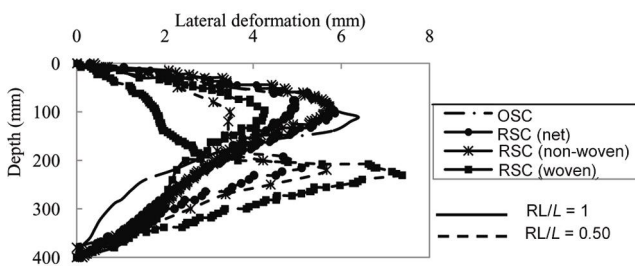


Figure 17. Lateral deformation versus depth for stone column reinforced with different types of reinforcement and reinforcement length, at a vertical settlement of 50 mm with ARR = 19.63%.

portions. Moreover, the lateral deformation for RSC (net) and RSC (non-woven) with RL/L = 1 near the top portion of the stone column is more than that with RL/L = 0.50. While for RSC (woven), the lateral deformation is more with RL/L = 0.50 (i.e. at the junction of reinforced and unreinforced portions) than with RL/L = 1. This may be due to transfer of larger stress at the junction of reinforced and unreinforced portions with higher stiffness of reinforcement.

Based on the numerical analyses on a limited group of reinforced stone columns, the following conclusions can be drawn.

The performance of a group of ordinary stone columns can be enhanced by providing suitable geosynthetic reinforcement.

With provision of full reinforcement, the load carrying capacity of a group of columns increases by 150% for the parameters adopted in the present study.

The stress concentration factor of a given group of reinforced columns is about 4.6 times more than a group of ordinary stone columns.

The lateral deformation of a reinforced stone column is reduced by 75%, compared to an ordinary stone column.

For partially reinforced stone column, lateral deformation is observed at the junction of reinforced and unreinforced portions of the stone column.

With increase in stiffness/modulus of reinforcement, load carrying capacity increases by two times for the values of stiffness considered in the current study.

The behaviour of partially reinforced stone column approaches to that of fully reinforcement stone column. In this study, bearing ratio is decreases by 14% as the length of reinforcement increase from 50% to 100% of the length of the column. This suggests that the stone column can be reinforced up to its partial length where lateral deformation is predominant.

1. Van Impe, W. F., *Soil Improvement Techniques and their Evolution*, Balkema, Rotterdam, The Netherlands, 1989, pp. 63–66.
2. Kempfert, H. G., Embankment foundation on geotextile-coated sand columns in soft ground. In Proceedings of the 1st European Geosynthetics Conference, Geosynthetics – applications, design and construction. Maastrich, The Netherlands, A.A. Balkema, Rotterdam, 1996, pp. 245–250.
3. Raithel, M., Kempfert, H. G. and Kirchner, A., Geotextile-encased columns (GEC) for foundation of a dike on very soft soils. In Proceedings of the 7th International Conference on Geosynthetics, France, 2002, pp. 1025–1028.
4. Bauer, G. E. and Nabil, A. J., Laboratory and analytical investigation of sleeve reinforced stone columns. In Proceedings of the First European Geosynthetics Conference, EUROGEO 1, Geosynthetics: application, design and construction, The Netherlands, 1996, pp. 463–466.
5. Malarvizhi, S. N. and Ilamparuthi, K., Load versus settlement of clay bed stabilized with stone and reinforced stone columns. In Proceedings of the 3rd Asian Regional Conference on Geosynthetics, Seoul, South Korea, 2004, pp. 322–329.

6. Trunk, G., Heerten, A., Poul, A. and Reuter, E., Geogrid wrapped vibro, stone columns. In EuroGeo3: Geotech. Eng. with Geosynthetics, Munich, Germany, 2004, pp. 289–294.
7. Ayadat, T. and Hanna, A. M., Encapsulated stone columns as a soil improvement technique for collapsible soil. *Ground Improvement*, 2005, **4**(9), 137–147.
8. Di Prisco, C., Galli, A., Cantarelli, E. and Bongiorno, D., Georeinforced sand columns: small scale experimental tests and theoretical modeling. In Proceedings of the 8th International Conference on Geosynthetics, Yokohama, Japan, 2006, pp. 1685–1688.
9. Lee, D., Yoo, C. and Park, S., Model tests for analysis of load carrying capacity of geogrid encased stone column. In the Proceedings of the 17th International Offshore and Polar Engineering Conference, Lisbon, Portugal, 2007, pp. 1631–1635.
10. Murugesan, S. and Rajagopal, K., Model tests on geosynthetic encased stone columns. *Geosynth. Int.*, 2007, **14**(6), 346–354.
11. Murugesan, S. and Rajagopal, K., Studies on the behavior of single and group of geosynthetic encased stone columns. *J. Geotech. Geoenviron. Eng.*, 2010, **136**(1), 129–139.
12. Murugesan, S. and Rajagopal, K., Shear load tests on stone columns with and without geosynthetic encasement. *J. Geotech. Testing*, 2008, **32**(1), 1–10.
13. Gniel, J. and Bouazza, A., Improvement of soft soils using geogrid encased stone columns. *Geotext. Geomembr.*, 2009, **27**(3), 167–175.
14. Wu, C. S. and Hong, Y. S., Laboratory tests on geosynthetic encapsulated sand columns. *Geotext. Geomembr.*, 2009, **27**(2), 107–120.
15. Gniel, J. and Bouazza, A., Construction of geogrid encased stone columns: a new proposal based on laboratory testing. *Geotext. Geomembr.*, 2010, **28**, 108–118.
16. Murugesan, S. and Rajagopal, K., Geosynthetic-encased stone columns: numerical evaluation. *Geotext. Geomembr.*, 2006, **24**(6), 349–358.
17. Malarvizhi, S. N. and Ilamparuthi, K., Comparative study on the performance of encased stone column and conventional stone column. *Soils Found.*, 2007, **47**(5), 873–885.
18. Khabbazian, M., Kaliakin, V. N. and Meehan, C. L., Numerical study of the effect of geosynthetic encasement on the behaviour of granular columns. *Geosynth. Int.*, 2010, **17**(3), 132–143.
19. Yoo, C. and Kim, S. B., Numerical modeling of geosynthetic encased stone column-reinforced ground. *Geosynth. Int.*, 2009, **16**(3), 116–126.
20. Yoo, C., Performance of geosynthetic-encased stone columns in embankment construction: numerical investigation. *J. Geotech. Geoenviron. Eng.*, 2010, **136**(8), 1148–1160.
21. Brinkgreve, R. B. and Vermeer, P. A., *PLAXIS 3D-Finite Element Code for Soil and Rocks Analysis*, A.A. Balkema, Rotterdam Brookfield, 2010.
22. Ambily, A. P. and Gandhi, S. R., Behavior of stone columns based on experimental and FEM analysis. *J. Geotech. Geoenviron. Eng.*, 2007, **133**(4), 405–415.
23. Mustafa, V., Mustafa, A., Banu, S., Ikizler, C. and Umit, C., Experimental and numerical investigation of slope stabilization by stone columns. *Nat. Hazards*, 2012, **64**, 797–820.

ACKNOWLEDGEMENT. We thank Mr Paresh Patel (Unique Construction, Surat) for providing financial support for the laboratory work.

Received 14 October 2014; revised accepted 15 December 2014

## On the vertical wavelength estimates using the Krassovsky parameters of OH airglow monitoring

R. N. Ghodpage<sup>1,\*</sup>, A. Taori<sup>2</sup>, P. T. Patil<sup>1</sup>,  
Devendraa Siingh<sup>3</sup>, S. Gurubaran<sup>4</sup> and  
A. K. Sharma<sup>5</sup>

<sup>1</sup>Medium Frequency Radar, Indian Institute of Geomagnetism, Shivaji University Campus, Kolhapur 416 004, India

<sup>2</sup>National Atmospheric Research Laboratory, Gadanki 517 112, India

<sup>3</sup>Indian Institute of Tropical Meteorology, Pune 411 008, India

<sup>4</sup>Indian Institute of Geomagnetism, Navi Mumbai 410 218, India

<sup>5</sup>Department of Physics, Shivaji University, Kolhapur 416 004, India

**The photometric measurements of mesospheric OH and O(<sup>1</sup>S) emission, carried out from Kolhapur (16.8°N, 74.2°E), Maharashtra during January–April 2005 are used to study the wave characteristics. The nocturnal variability reveals the dominant long-period wave signatures with significant amplitudes of embedded short-period waves. We carry out a sensitivity study on the vertical wavelength (VW) derived with the help of Krassovsky parameters ( $\eta = |\eta|e^{i\phi}$ ) of the OH data, which reveals VW to vary from 38.9 to 110.2 km. This was compared with the VW estimates using the phase difference of the simultaneously observed waves in both OH and O(<sup>1</sup>S) emission intensities. Results reveal that in the absence of attitudinally resolved measurements, the VW estimated using Krassovsky method can be used.**

**Keywords:** Airglow, atmospheric gravity waves, lower thermosphere, mesosphere, vertical wavelength.

ATMOSPHERIC gravity waves (AGWs) play a significant role in the dynamics features of the mesosphere and lower thermosphere (MLT) region by transporting energy and momentum horizontally and vertically upward and also providing dynamical linkage between the lower atmosphere and the MLT region. Multispectral nightglow emissions recorded at low-latitude stations showed the presence of gravity waves with periods ranging from a few minutes to a few hours<sup>1,2</sup>. Ground-based airglow emissions are widely used to study the short-period (tens of minutes) waves with short horizontal wavelength (tens of kilometres)<sup>3–7</sup>. Hecht *et al.*<sup>8</sup> showed the presence of long-period (~2 h) and large horizontal wavelength (~300–400 km) gravity waves as well as short-period (15–25 min) and small horizontal wavelength (~30–45 km) gravity waves in the airglow data over Alice Spring, Australia. The short-period waves might have been trapped/ducted by thermal ducts and took several hours to reach the mesopause region. Snively *et al.*<sup>7</sup> reported that airglow perturbations of small-scale ducted gravity waves near the Brunt–Vaisala period are primarily

\*For correspondence. (e-mail: rupeshghodpage@gmail.com)